Pharm Res (2014) 31:1106–1119
DOI 10.1007/s11095-013-1234-x

RESEARCH PAPER

Multicompartimental Nanoparticles for Co-Encapsulation and Multimodal Drug Delivery to Tumor Cells and Neovasculature

Lívia Palmerston Mendes • Marilisa Pedroso Nogueira Gaeti • Paulo Henrique Marcelino de Ávila • Marcelo de Sousa Vieira • Bruna dos Santos Rodrigues • Renato Ivan de Ávila Marcelino • Lílian Cristina Rosa dos Santos • Marize Campos Valadares • Eliana Martins Lima

Received: 26 July 2013 / Accepted: 14 October 2013 / Published online: 30 October 2013

ABSTRACT

Purpose The purpose of this work was the development of a multicompartimental nanocarrier for the simultaneous encapsulation of paclitaxel (PTX) and genistein (GEN), associating antiangiogenic and cytotoxic properties in order to potentiate antitumoral activity.

Method Polymeric nanocapsules containing PTX were obtained by interfacial deposition of preformed polymer and coated with a phospholipid bilayer entrapping GEN. Physical-chemical and morphological characteristics were characterized, including size and size distribution, drug entrapment efficiency and drug release profile. *In vivo* studies were performed in EAT bearing Swiss mice.

Results Entrapment efficiency for both drugs in the nanoparticles was approximately 98%. Average particle diameter was 150 nm with a monomodal distribution. *In vitro* assays showed distinct temporal drug release profiles for each drug. The dose of 0.2 mg/kg/day of PTX resulted in 11% tumor inhibition, however the association of 12 mg/kg/day of GEN promoted 44% tumor inhibition and a 58% decrease in VEGF levels.

Conclusions Nanoparticles containing GEN and PTX with a temporal pattern of drug release indicated that the combined effect of cytotoxic and antiangiogenic drugs present in the formulation contributed to the overall enhanced antitumor activity of the nanomedicine.

KEY WORDS antiangiogenesis · antitumoral · co-encapsulation · multicompartimental nanoparticles · temporal drug release

L. P. Mendes • M. P. N. Gaeti • L. C. R. dos Santos • E. M. Lima (✉)
Laboratório de Nanotecnologia Farmacêutica e Sistemas de Liberação de Fármacos–FarmaTec, Faculdade de Farmácia
Universidade Federal de Goiás, Goiânia, GO, Brazil
e-mail: emlima@farmacia.ufg.br

P. H. M. de Ávila • M. de Sousa Vieira • B. dos Santos Rodrigues • R. I. de Ávila Marcelino • M. C. Valadares
Laboratório de Farmacologia e Toxicologia Celular–FarmaTec–Faculdade de Farmácia Universidade Federal de Goiás, Goiânia, GO, Brazil

ABBREVIATIONS

BS	Backscattering
CCT	Capric/caprylic triglyceride
EAT	Ehrlich ascites tumor
EE	Encapsulation efficiency
FDA	Food and drug administration
GEN	Genistein
HPLC	High performance liquid chromatography
i.p.	Intra peritoneal
NC	Uncoated nanoparticles
NC-PC	Coated nanoparticles
NP	Nanoparticles
NTA	Nanoparticle tracking analysis
PBS	Phosphate buffered saline
PdI	Polydispersity index
PLGA	Poly(lactic-co-glycolic acid)
PTX	Paclitaxel
PVDF	Polyvinylidene difluoride
SLS	Sodium lauryl sulfate
T	Transmission
TEM	Transmission electron microscopy
VEGF	Vascular endothelial growth factor

INTRODUCTION

Cancer treatment usually associates antitumor agents with different mechanisms in order to improve chemotherapy efficacy and minimize adverse effects (1,2). Among chemotherapeutic agents, paclitaxel (PTX) is currently widely used due to its cytotoxic properties against solid tumors (3,4). However, the toxicity of the current vehicle used to administer this drug (Cremophor EL) associated with the need of administration of high doses of PTX might jeopardize a successful clinical outcome of the treatment (5).

To circumvent these disadvantages, Cremophor-free formulations are being developed and the FDA has already approved a nanoparticle formulation of albumin-bound paclitaxel for the treatment of breast cancer after failure of combination chemotherapy for the metastatic form of the disease. Several studies have investigated the role of these nanoparticles as a single agent and in combination with other drugs for the treatment of different types of solid tumors (6–8). The combination of PTX with angiogenic inhibition factors such as bevacizumab has proven an increase in the antineoplastic effect due to the association of these drugs without an increase in side effects (9,10). The co-encapsulation of PTX combined with other drugs in nanocarriers may also be a promising strategy to increase therapeutic effects, also reducing side effects (11,12).

Nanostructured polymeric and lipid-based systems may improve the biological response to many molecules, especially by modulating their pharmacokinetics and thus resulting in numerous advantages such as reduced toxicity and controlled release of the drugs. For a sustained release, different kinds of polymers or lipids, such as polydiacetylene, phospholipids and poly(ε-caprolactone) derivatives, may be used to modulate the release of the drug, maintaining its plasmatic concentration in therapeutic levels, during a prolonged period of time (13,14).

Recent approaches focusing on the development of a nanocarrier system co-encapsulating two antineoplastic drugs include the use of liposomes and polymer nanoparticles whose antitumor activity result from the association of different drugs in a lower dose than the ones used in conventional therapy, overcoming undesirable toxicity and avoiding multidrug resistance (MDR) (15–17). The association of a cytotoxic drug with drugs that act on tumor angiogenesis is a distinct strategy, since antiangiogenic drugs do not act directly in the elimination of the tumor, but inhibit the growth of a vascular system surrounding the tumor, thereby preventing the influx of oxygen and nutrients (18–20). Therapeutic potential of this approach has been shown for the combination of a vasculature disrupting agent, combrestatin A4, and the cytotoxic drug paclitaxel in nanoparticles, which resulted in inhibition of tumor cell proliferation and neovasculature growth (21).

Genistein (GEN), one of the major isoflavones found in soy extracts, is among new molecules used for the inhibition of tumor angiogenesis. It has shown potential antitumoral activities by its antiangiogenic effect in preventing cell proliferation and avoiding the occurrence of metastasis (22,23). GEN antiangiogenic and antitumor effects have been recently elucidated and involves, among other mechanisms, the inhibition of the vascular endothelial growth factor (VEGF), a molecule widely found in animal and human tumors (22,24). However, a known paradox of the antiangiogenic therapy is that the reduced blood supply induces tumor hypoxia, leading to the activation of factor which can significantly reduce the pro-apoptotic effect of chemotherapy, leading to tumor resistance (25). As a result, the association of GEN with other cytotoxic drugs already used in antineoplastic therapy is required, in order to increase the antitumor activity, avoiding the occurrence of MDR cancer cells (26–28).

Given this scenario, the association of PTX and GEN in a nanostructured drug delivery system may lead to a synergic effect. The immediate release of the antiangiogenic drug combined with the sustained release of the cytotoxic agent might potentiate the antitumor activity. Thus, the aim of this work was to develop, characterize and evaluate tumor inhibition *in vivo* of a nanomedicine comprising multicompartimental nanoparticles co-encapsulating GEN and PTX with a temporal pattern of drug release.

MATERIALS AND METHODS

Material

Paclitaxel (PTX) and genistein (GEN) were acquired from LC Laboratories (Woburn, MA, USA). Poly(lactic-co-glycolic acid) (PLGA) 75:25 was purchased from BoehringerIngelheim (Ingelheim, Germany). Capric/caprylic triglyceride (CCT) was a gift from ABITEC (Columbus, OH, USA) and soy phosphatidylcholine (PC) was obtained from LIPOID (Ludwigshafen, Germany). Pluronic® F68 and F127 (poloxamer) were purchased from Sigma-Aldrich (St. Louis, MO, USA). Acetonitrile HPLC grade and trifluoroacetic acid were acquired from JT Baker (Phillipsburg, NJ, USA). Ultra-purified water was used and all other chemicals were of analytical reagent quality.

HPLC Analysis

Reversed-phase HPLC was used for the quantitative determination of GEN and PTX in all samples. The system used was a Varian Pro Star Chromatographer (USA) equipped with an autosampler model PS410, UV-Visible detector model PS325 and a quaternary pump model PS240. Chromatographic separation was achieved in a C18 column packed with OmniSpher 3 ODS silica, with 50 mm length by 3.0 mm internal diameter (Varian, USA) at room temperature. Solvent A was Milli-Q purified water containing 0.1% (v/v) trifluoroacetic acid, and solvent B was acetonitrile HPLC grade. The solvents were pumped through the system at a flow rate of 0.5 mL/min. A mobile phase gradient was used, starting at 65% solvent A for 0.5 min, decreasing to 20% at 1 min and returning to the initial condition until the end of analysis (5 min). In order to increase the detection sensitivity of each drug, wavelength was set at 260 nm for GEN and 227 nm for PTX. Elution time for GEN was 2.10 min while

PTX eluted at 3.70 min. PTX and GEN quantifications were carried out using external standard calibration curve in the linear concentration range between 1 and 100 μg/mL. The limit of detection (LD), defined as the lowest concentration of the analyte which can be detected but not necessarily quantitated, was 0.04 μg/mL for GEN and 0.06 μg/mL for PTX. While the limit of quantification (LQ) was 0.13 μg/mL for GEN and 0.2 μg/mL for PTX.

Preparation of Nanoparticles

PTX-loaded PLGA nanocapsules coated with a lipid bilayer containing GEN were denoted in this work by NC-PC and were prepared as follows. Nanocapsules of PLGA 75:25 containing PTX were prepared by interfacial deposition of preformed polymer. Briefly, PLGA and CCT were dissolved in acetone. PC and PTX (2.5 mg) were dissolved in methanol and mixed with the acetone solution. The aqueous solution was prepared using Pluronic® F68 and F127 (1:1) at 0.37% (w/v). The organic solution was dripped into the aqueous solution under magnetic stirring, which was maintained for 30 min. After that period, the solvents were evaporated under reduced pressure at 40°C and 45 rpm in a rotary evaporator (Ika, Germany) during which the nanocapsules were formed. Non-encapsulated drug was removed by filtration using a 0.45 μm PVDF membrane.

PC and GEN (2.5 mg) were dissolved in a mixture of chloroform and methanol. A thin lipid film was prepared by the evaporation of the organic solvents in a nitrogen atmosphere. The flask was kept under vacuum (440/2D, Nova Ética, Brazil) for 1 h to ensure complete removal of residual solvent. The thin-film was hydrated for 1 h using the dispersion of polymeric nanocapsules prepared as previously described. At the end of the procedure, samples were filtered through 0.45 μm membrane, which also removed the non-encapsulated genistein. Blank nanoparticles (without drugs) were also obtained for control purposes.

Nanoparticles Characterization

Nanoparticles were characterized after both steps described above. The size distribution profiles were determined by dynamic light scattering (DLS) in a Zetasizer Nano S (Malvern Instruments, UK), with the sample previously diluted in ultrapure water. Analysis of pH was done directly in the pH meter PG 1800 (Gehaka, Brazil).

Morphological examination of nanoparticles was performed by transmission electron microscopy (TEM) by negative staining with 2% (w/v) uranyl acetate solution and examined in a Jeol JEM-2100 Electron Microscope (Jeol, Tokyo, Japan) operating at 100 kV. One droplet of the nanoparticles dispersion was placed on a formvar coated copper grid (400 mesh). After 1 min at room temperature, the excess liquid was removed using filter paper. For negative staining, the sample on the grid was covered with one drop of uranyl acetate (2% w/v) for 2 min. Excess of uranyl acetate was removed and grids were allowed to dry at room temperature for at least 30 min.

Quantitative determination of encapsulated drugs was performed by HPLC as previously described. For the HPLC analysis, 100 μL aliquots of the sample before and after filtration were diluted with 900 μL of methanol to disrupt the nanoparticles. These aliquots were centrifuged at 14,500 rpm (MiniSpin plus, Eppendorf, Germany) for 10 min and the supernatant was injected into the chromatographer. Encapsulation efficiency (EE) for both drugs was calculated from the following equation:

$$\%\mathrm{EE} = \frac{amount\ \ of\ \ drug\ \ encapsulated(mg)}{amount\ \ of\ \ drug\ \ added\ \ to\ \ formulation(mg)} \times 100$$

All samples were prepared in triplicates and analysis were performed in three different batches ($n = 3$).

Nanoparticle Tracking Analysis

Nanoparticle tracking analysis (NTA) is a method of visualizing and analyzing particles in liquids that relates the rate of Brownian motion to particle size. Particles are visualized by the light scattered when illuminated by a laser light. The technique calculates particle size on a particle-by particle basis. Videos of the light scattered by the particles are captured using a digital camera and the motion of each particle is tracked from frame to frame. The rate of particle movement is related to a sphere equivalent hydrodynamic radius as calculated through the Stokes-Einstein equation (29). NTA measurements were performed with a NanoSight NS500 (Amesbury, United Kingdom), equipped with a sample chamber and a 532-nm laser. Samples of uncoated and coated nanocapsules were diluted before analysis with ultrapure water and automatically loaded into the sample chamber. The software used for capturing and analyzing the data was the NTA 2.3. Video clips of the samples were captured by an EMCCD camera for 215 s with manual shutter and gain adjustments. The mean size and SD values obtained by the NTA software correspond to the arithmetic values calculated with the sizes of all the particles analyzed by the software. All measurements were performed at room temperature.

A blank liposomal dispersion prepared with 25 mM phosphatidylcholine was prepared by the hydration of a thin-lipid film method followed by vigorous agitation and extrusion (LIPEX Extruder, Northern Lipids, Canada) through a polycarbonate membrane of 600 nm. These liposomes were analyzed by NTA and DLS. An aliquot of this sample was mixed with an aliquot of uncoated nanocapsules and also

analyzed by NTA and DLS in order to compare the size and size distribution of the lipid vesicles formed in the absence of the nanocapsules and the NC-PC nanoparticles.

Multiple Light Scattering Analyses

Nanoparticles were analyzed by multiple light scattering (MLS) using Turbiscan Lab Expert (Formulaction, France) before and after coating with lipid bilayer. The sample was placed in a cylindrical glass cell and analyzed for 24 h at 25°C. The equipment consisted of a detection head with a pulsed near infra-red light source ($\lambda = 880$ nm) which moves along the glass cell. This detection head is also equipped with a synchronous transmission (T) and back scattering (BS) detectors. The T detector receives the light which goes across the sample (at 180°) and the BS detector receives the light scattered backward by the sample (at 45°) (30). The detection head scans the entire height of the sample acquiring T and BS data simultaneously every 40 μm and each 20 min during 24 h of analysis.

In Vitro Drug Release

500 μl of drug loaded nanoparticles dispersion were added to a dialysis tube (MW cut off 3500 D) and sealed. The tube was immersed in 10 mL of acceptor medium prepared with sodium lauryl sulfate (SLS) 2.0% (w/v). The flasks were maintained in an orbital shaker (Marconi, Brazil) at 37°C at 125 rpm for 60 days. Samples were withdrawn from the acceptor medium and replaced by fresh medium at predetermined time points. Samples were injected directly in the HPLC system to determine the amount of drugs released from the nanoparticles. The procedure was performed in triplicate and sink conditions were maintained during the experiment. To ensure sink conditions, solubility of both drugs was assessed in several SLS concentrations during 24 h at 37°C in the orbital shaker. Samples were then filtered in a 0.45 μm membrane, diluted in methanol and analyzed by HPLC.

In Vivo Assay

Animals

Groups of 6–8 week-old Swiss male mice from the Institute of Biological Sciences of University Federal of Goias were used. The animals weighing 30–35 g at the beginning of the experiment were housed under the conditions of controlled temperature (26°C ± 2°C) and light (12 h light/12 h dark) and received food and water *ad libitum*. The experiment was conducted according to the protocol number 37/2009 approved by the UFG Ethics Committee for Animal Studies.

Tumor Model

Ehrlich Ascites Tumor (EAT) was maintained in the ascitic form by sequential passages in Swiss mice, by means of intra peritoneal (i.p.) transplantations of 2×10^6 tumor cells. The ascitic fluid was collected using a syringe and tumor cell count was performed in a Neubauer hemocitometer, using the trypan blue dye exclusion method.

Tumor Inhibition

Animals were separated into 8 groups of 5 animals each. Each animal used in the assay was inoculated i.p. with 2×10^6 tumor cells suspended in 0.2 mL of phosphate buffered saline (PBS) solution (pH 7.4). The date of tumor inoculation was consider day 0 and the administration of nanoparticles started at day 1. To evaluate tumor inhibition, NC-PC formulations containing PTX+GEN or PTX or GEN, at different concentrations of each drug were prepared. EAT-bearing mice were treated i.p. during 7 consecutive days with different doses of the drugs following the protocol for each group: GEN+PTX 12+10 mg/kg/day (G12P10); PTX 10 mg/kg/day (G0P10); GEN+PTX 12+2 mg/kg/day (G12P2); PTX 2 mg/kg/day (G0P2); GEN+PTX 12+0.2 mg/kg/day (G12P0.2); PTX 0.2 mg/kg/day (G0P0.2); GEN 12 mg/kg/day (G12P0); Blank nanoparticles (control group, C).

Animals were submitted to euthanasia on the eighth day of the experiment and the ascitic fluid was collected and centrifuged for 5 min at 1,500 rpm (3–18K, Sigma, Germany). The supernatant was reserved for the quantitation of VEGF and the pellet was ressuspended in PBS solution for the counting of tumor cells using the trypan blue dye exclusion method. C group (treated with blank nanoparticles) was the control group and its cell viability was considered 100%.

Determination of VEGF in Ascitic Fluid

Levels of VEGF from the peritoneal washing supernatant of EAT-bearing mice from groups G12P2, G0P2, G12P0.2, G0P0.2, G12P0 and C were determined by an ELISA Kit (Mouse VEGF Quantikine ELISA Kit) using a quantitative sandwich enzyme immunoassay technique. The ascitic fluid was subjected to the test in duplicate following manufacturer instructions (R&D systems). In brief, 50 μL of assay diluent and 50 μL of samples previously diluted were added to a 96-well microplate pre-coated with polyclonal antibody specific for mouse VEGF. Recombinant mouse VEGF was used to set up the standard curve. After incubation for 2 h at room temperature, the wells were washed and polyclonal antibody against mouse VEGF conjugated to horseradish peroxidase was added. Incubation was continued for 2 h and plates were washed again. Substrate solution was added

to each well and incubated for 30 min. The enzyme reaction yielded a blue product that turns yellow when the stop solution is added. The optical density (O.D.) was measured at 450 nm and 540 nm using a microplate reader MultiskanSpctrum (Thermo Scientific, EUA). Readings at 540 nm were subtracted from the readings at 450 nm to correct for optical interferences from the plate.

Macroscopic Evaluation of Antiangiogenic Effect

At the end of the treatment, the peritoneal wall from the abdominal region of mice were carefully collected to verify angiogenesis. For this assay, photographs of a defined area were taken by a digital camera (Sony, Japan) and a macroscopic morphologic analysis was accomplished (31). Image J was used to convert grey scale images into 8-bit binary images. The area of blood vessels from the peritoneum was selected and the number of positive pixels/mm^2 was determined.

Statistical Analysis

In vivo experiments were performed in quintuplicate and results were expressed as mean ± SD. For comparison of mean values between groups, Analysis of Variance test (ANOVA) and Tukey's Multiple Comparison test were used. In all cases, statistical difference was accepted when $p < 0.05$. Statistical analyzes were performed using GraphPad Prism software (version 5.0).

RESULTS

Preparation and Characterization of Nanoparticles

PLGA nanocapsules encapsulating PTX were prepared by the interfacial deposition of preformed polymer method. The formation of the PC envelope was accomplished in a second stage, by hydrating the phospholipid film containing genistein with the nanocapsules dispersion. The phospholipid bilayer coating was designed in order to encapsulate GEN and promote a faster release of this drug in contrast with the polymeric core of these nanoparticles. Schematic representation of the particle is presented in Fig. 1. Final formulation had an opalescent and whitish aspect.

Physical-chemical characteristics of the nanoparticles are presented in Table I. Both nanoparticle dispersions (NC and NC-PC) exhibited a monomodal size distribution and polidispersity around 0.1, indicating narrow size distributions. Following the hydration of the phospholipid film with the dispersion of nanocapsules, the visual aspect of the formulation remained unaltered. The mean diameter of the phospholipid coated nanoparticles increased approximately 21% (about 25–30 nm). The multicompartimental nanoparticles also exhibited a monomodal size distribution with a similar size distribution profile in comparison to the uncoated nanocapsules.

Dynamic light scattering measurements of the formulations were plotted as intensity, volume and number for all samples (Fig. 2). Results show that the formulations were monodisperse, with a high homogeneity and narrow size distribution, as demonstrated by almost superposed size distribution profiles in different plots of singular batches. Nanoparticles were visualized by transmission electron microscopy after negative staining with uranyl acetate and the spherical shape and uniformity of drug loaded NP was confirmed after both stages of preparation (Fig. 3). It was also possible to observe the surrounding bilayer around the polymeric nanocapsules, confirming the enclosure of NC by the PC envelope.

HPLC chromatograms in Fig. 4 demonstrate that NC-PCs had the characteristic peaks of the free drugs, confirming that both drugs were encapsulated in the nanoparticles. Encapsulation efficiencies for GEN and PTX were 98% and 97.8%, respectively, resulting in NC-PC formulations containing 0.51 ± 0.10 mg/mL of PTX and 0.61 ± 0.18 mg/mL of GEN.

Nanoparticle Tracking Analysis

With the purpose of confirming the results obtained by DLS that suggested the obtention of PC-coated nanocapsules, samples were analyzed by NTA technique (Fig. 5). Both uncoated (NC) (Fig. 5a) and coated (NC-PC) (Fig. 5b) nanoparticles exhibited only one population of particles, and no other particles in a different size range were observed. Additionally, the column charts on the left side in Fig. 5 demonstrate a good agreement between NTA and DLS results, with relatively narrow size distributions for all formulations. To ensure that NC-PC formulations were not a mixture of nanocapsules and phospholipid vesicles, liposomes were obtained as described above and mixed with an aliquot of uncoated nanocapsules. DLS analyses of these liposomes before the mixture presented a mean size diameter of 517 nm and PdI of 0.04, in agreement with NTA, which showed only one population of vesicles with a mean diameter of 587 nm and a SD of 87 nm (Fig. 5c). When liposomes were mixed with nanocapsules, DLS still showed only one population of nanoparticles with an average diameter of 185 nm with a PdI of 0.26, while NTA clearly showed two populations of particles, noticeably in a different size distribution range (Fig. 5d).

Multiple Light Scattering

The backscattering profile of the nanocapsules dispersion before and after the lipid coating is presented in reference mode (Fig. 6), in which the first profile is subtracted from the other profiles. A discrete increase (about 2%) in the backscattering, both in the top and in the bottom of the

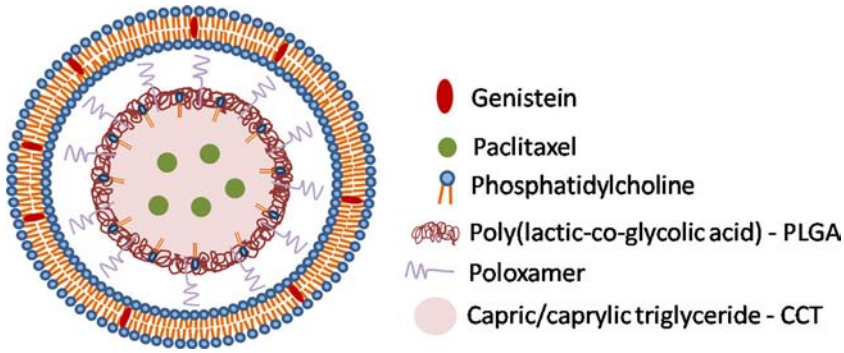

Fig. 1 Schematic illustration of the formulation of nanocapsules coated with a phosphatidylcholine bilayer (NC-PC) containing both paclitaxel and genistein–NCs comprise a capric/caprylic triglyceride core, a poly(lactic-co-glycolic acid) shell and a phospholipid bilayer coating.

sample, after coating were observed, indicating that the concentration of the particles is increasing in these areas of the sample cell. This observation is an estimative of sedimentation and creaming behaviors. Before coating, a more discrete variation can be observed only in the top region of the sample. Nevertheless, no variation can be seen in the middle of both samples, indicating that there is no change in particle size. This indicates that particles are not coalescing or flocculating while they migrate to the top or the bottom of the sample.

In Vitro Drug Release

The *in vitro* drug release profiles of PTX and GEN during 60 days are shown in Fig. 7. It can be observed that GEN is completely released during the initial 48 h of the test, while PTX shows only a 10% release in the same time. The difference between the total amount of GEN and the amount quantified in the receptor medium (about 85%) results from the equilibrium reached between donor and receptor compartments after the complete release of the drug. After 60 days of analysis, almost 70% of PTX was released from nanoparticles. Solubility of PTX and GEN in the receptor medium (SLS 2.0%) was 672.65 ± 7.76 and 217.78 ± 8.82 μg/mL, respectively, ensuring sink conditions for the drug release assay. A noticeable temporal drug release pattern was observed. GEN entrapped in the surrounding lipid envelope of the nanoparticles was promptly released when compared to the sustained release of PTX encapsulated in the internal compartment of the polymeric core of these multicompartimental nanostructured systems.

In Vivo Assay

Each group of mice were treated with different nanoparticles formulations for up to 7 days. At the dose of 10 mg/Kg/day of PTX, there was 95% and 96% tumor growth inhibition for groups G12P10 and G0P10, respectively, as shown in Fig. 8. However, animals presented diarrhea and about 20% of weight loss at the end of the test, compared to their weight at the beginning of the test. With a 5-fold decrease in the dose of PTX in groups G12P2 and G0P2, tumor growth inhibition was 89%, similar to results found in groups G12P10 and G0P10 ($p > 0.05$). In addition, animals from these groups did not show toxicity signals.

Group G0P0.2 receiving a dose of 0.2 mg/Kg/day (50 times lower than the established dose) of PTX showed only 11% tumor growth inhibition. However, group G12P0.2, in which 12 mg of GEN were added, presented 44% of tumor growth inhibition. This data implicate that the association of a low dose of PTX and GEN can significantly impact tumor growth inhibition.

Comparing ascitic fluid levels of VEGF, it was possible to see in Fig. 9 a significantly reduction on tumor levels of VEGF

Table I Physical-Chemical Characteristics of the Paclitaxel-Loaded PLGA Nanocapsules (NC) Uncoated and Coated with a Phospholipid Bilayer Containing Genistein (NC-PC)

Nanoparticle	Diameter (nm)	PdI	pH	E.E. %[a]
Uncoated PLGA nanocapsules (NC)	125.07 ± 7.09	0.10 ± 0.02	6.15 ± 0.49	97.80 ± 1.65 (PTX)
PLGA nanocapsules coated with PC bilayer (NC-PC)	151.53 ± 5.64	0.17 ± 0.03	6.45 ± 0.35	97.80 ± 2.21 (PTX) 97.99 ± 2.90 (GEN)

Results express the mean ± SD ($n = 3$)

PC phosphatidylcholine; *PdI* polydispersity index; *E.E.* entrapment efficiency; *PTX* paclitaxel; *GEN* genistein

[a] EE% represents the amount (%) of encapsulated drug in relation to the total amount of drug added to the formulation *(EE% = (mg encapsulated drug)/(mg drug added to formulation) × 100)*

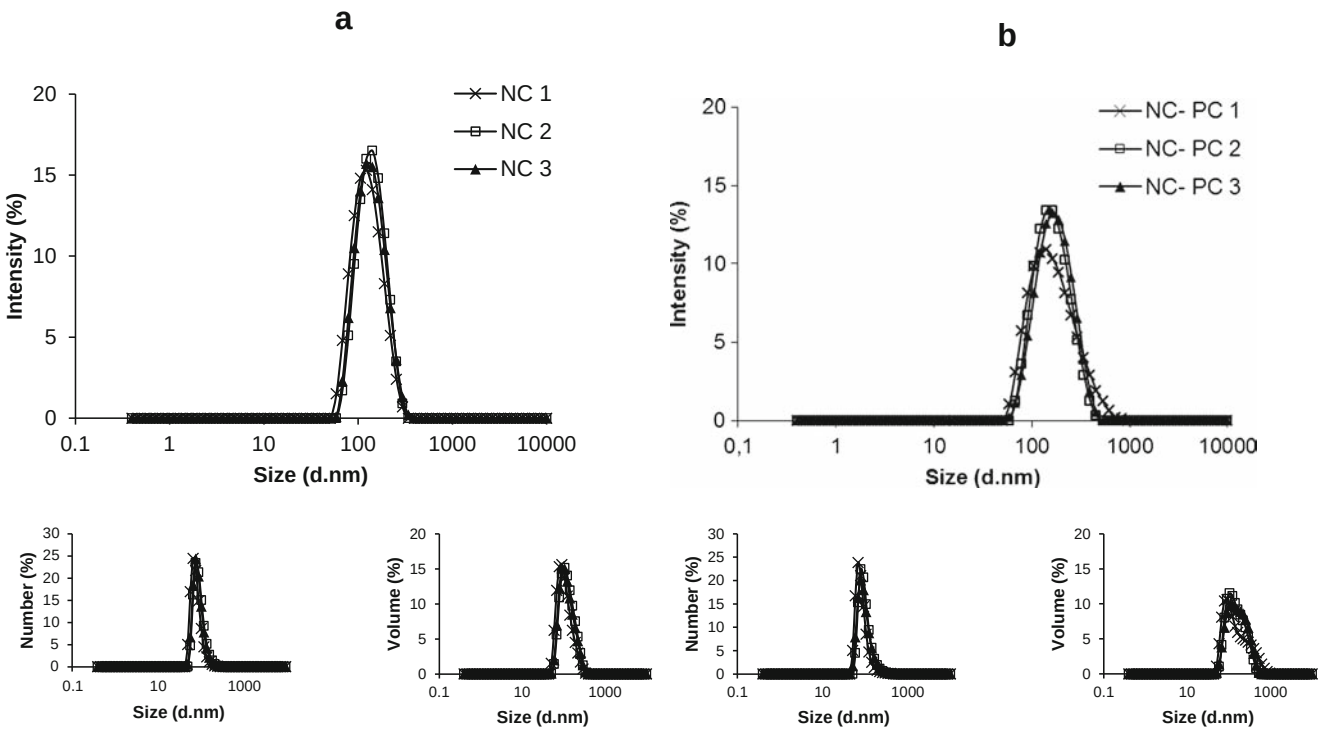

Fig. 2 Size distribution profiles by Dynamic Light Scattering considering light intensity, number, volume and particle size for the uncoated NCs (**a**) and after (**b**) coating the nanocapsules with the lipid bilayer. Each graph shows the measurement of three separate batches.

($P<0.05$) between the control group and G12P0.2. The presence of GEN reduced the amount of this cytokine by 58%. As there was a high tumor inhibition in groups G12P2 and G0P2, less than 2 ng of VEGF were quantified in the tumor.

Macroscopic analysis of the peritoneal wall of EAT-bearing mice (Fig. 10) allows the observation of visible changes in peritoneal vessels among different treatment protocols. The vessels were increased in number with a tortuous aspect, congested with erythrocytes and were highly dilated in EAT-bearing mice treated only with blank nanoparticles (Fig. 10b). The group where GEN was added to the treatment (Fig. 10d) presented lower density of vessels, which were not as congested or tortuous as PTX-only (Fig. 10c) and control

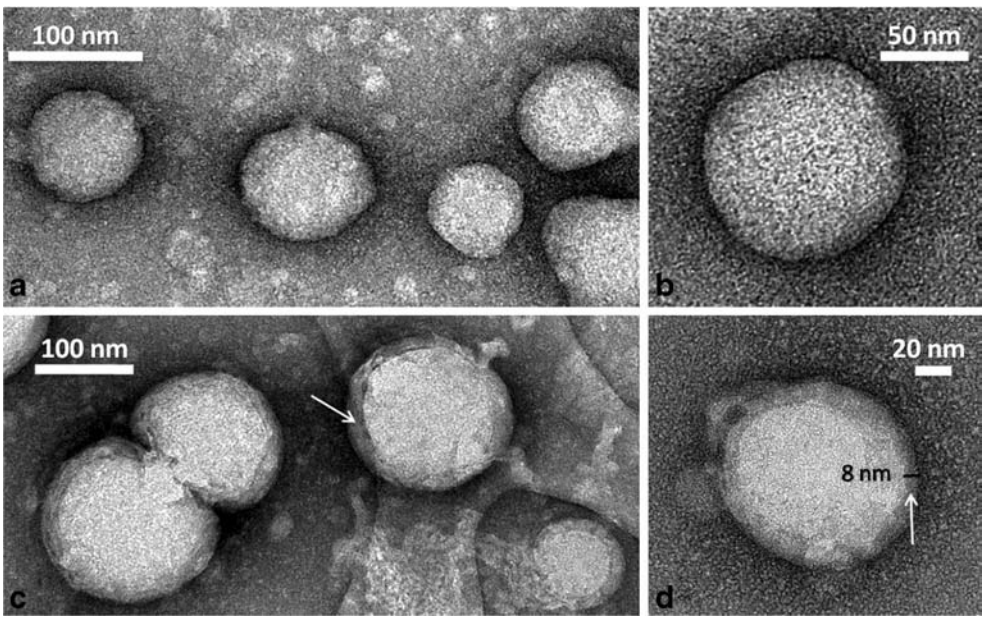

Fig. 3 Transmission electron micrograph of nanoparticles after negative staining with uranyl acetate. (**a**, **b**) Polymeric nanocapsules (NC) and (**c**, **d**) Polymeric nanocapsules coated with a phospholipid bilayer (NC-PC), confirming the presence of a surrounding lipid envelope around NC (*white arrows*) after the hydration of the phospholipid film with the NC dispersion.

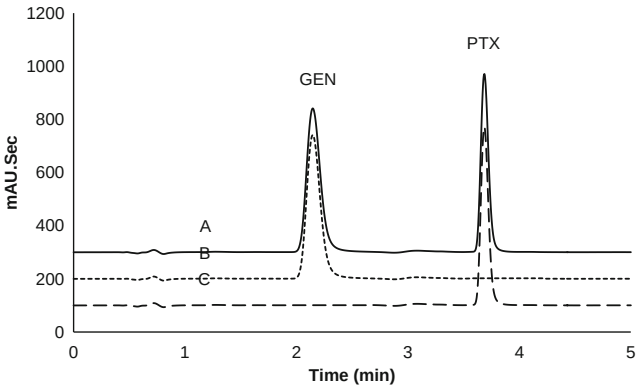

Fig. 4 HPLC chromatograms of (**a**) genistein (GEN), (**b**) paclitaxel (PTX) and (**c**) phospholipid coated nanocapsules (NC-PCs)containing both drugs. Samples were diluted (100 μg/mL) in methanol. Chromatographic conditions included a C18 column (50 × 3.0 mm; 3 μm); mobile phase was 0.1% trifluoroacetic acid solution in water/acetonitrile in gradient elution. Detection was UV at 260 nm for GEN and 227 nm for PTX.

groups, indicating its antiangiogenic effect, already shown by the evaluation of the presence of VEGF. Also, Image J analysis confirms a higher intensity of red from blood vessels in the control and G0P0.2 groups compared to G12P0.2.

DISCUSSION

In this work, a nanostructured drug delivery system for the co-encapsulation of PTX and GEN was developed and characterized, and a different time release pattern for each drug was accomplished. Advantages and synergic effects of the combination of antiangiogenic and cytotoxic drugs have been demonstrated by several studies (32–34), however there are no reports in the literature of the association of PTX and GEN in nanostructured drug delivery systems. The encapsulation of PTX, a classical cytotoxic agent, in nanocarriers has been widely studied and presents many advantages over conventional formulations (13,35,36). Conversely, very few reports are available applying nanotechnology to formulations with GEN, which also exhibits cytotoxic effects and a marked antiangiogenic activity (37–39).

Multicompartimental nanoparticles encapsulating both PTX and GEN were obtained with high encapsulation efficiency for both drugs, average diameter of approximately 150 nm and narrow size distribution. The inner core of the nanoparticles, represented by polymeric nanocapsules containing PTX presented a mean diameter of near 125 nm. Following their coating by lipid bilayers entrapping GEN, DLS measurements indicated an increase of approximately 25 nm, which is consistent with the thickness of lipid bilayers (40–42). Phospholipid bilayers assembled on the surface of the nanocapsules probably via hydrophilic interactions between the hydrophilic fraction of the surfactants in the water/polymer interface on the surface of the nanocapsules and the polar head group of the phospholipids. This process could be assumed since the DLS analysis showed a slight increase in diameter, maintaining a monomodal distribution, proved by the NTA analysis, which did not show any other population in different size distribution ranges after the lipid film envelope was formed. Also, TEM imaging was performed to ensure the presence of the envelope surrounding the nanocapsules, which presented an average thickness of 8 nm (determined using the scale bar provided by the TEM instrument). The imaging results shown in Fig. 3 reveal a spherical morphology and overall agreement in size compared to the size information obtained from light scattering analyses.

When liposomes of about 600 nm were prepared and mixed with uncoated nanocapsules, the presence of two nanoparticle populations, with distinct size distribution profiles, was observed. The NTA data clearly demonstrated the existence of two different populations of particles in the sample, with different light scattering intensities, showing that the previously formed liposomes did not interact with the polymeric nanoparticles. These data support the hypotheses that PTX-loaded nanocapsules acted as a template for the assembling and deposition of the phospholipid bilayer containing GEN.

Variations of the backscattered (ΔBS) light obtained in this work remained within ±2% of the ΔBS scale, indicating the stability of the nanomedicine formulation, since no variation in particle diameter was observed. Multiple light scattering analysis is a valuable tool in estimating the stability of disperse systems. Data indicated very mild sedimentation and creaming phenomena and in a very slow rate, both easily reversible. Variations greater than 10% of the BS are indicative of formulation instability, typical from formulations with marked differences between disperse and continuous phases, which could compromise formulation homogeneity (43,44).

A temporal drug release profile for each drug was observed. As GEN is entrapped in the outer lipid bilayer, it was completely released in the first 48 h of the assay. Partition of drugs into phospholipid membranes depends on their solubility and is driven by hydrogen bonds or van der Waals interactions between the hydrophobic drug and the phospholipids hydrophobic chains in the bilayer (45,46). The reversibility of the phospholipid-drug interaction, leading to the release of the entrapped drug, plays an important role in the drug elution process, which may vary from a few minutes to a few days. Lipid membrane composition and drug lipophilicity strongly influence drug release (47). The fast release of genistein from the phospholipid envelope of the NC-PCs might result from the lipid dynamics in the membrane, changing its binding sites very rapidly, despite its lipophilicity. Additionally, no electrostatic interactions were present, since both membrane phospholipids and genistein

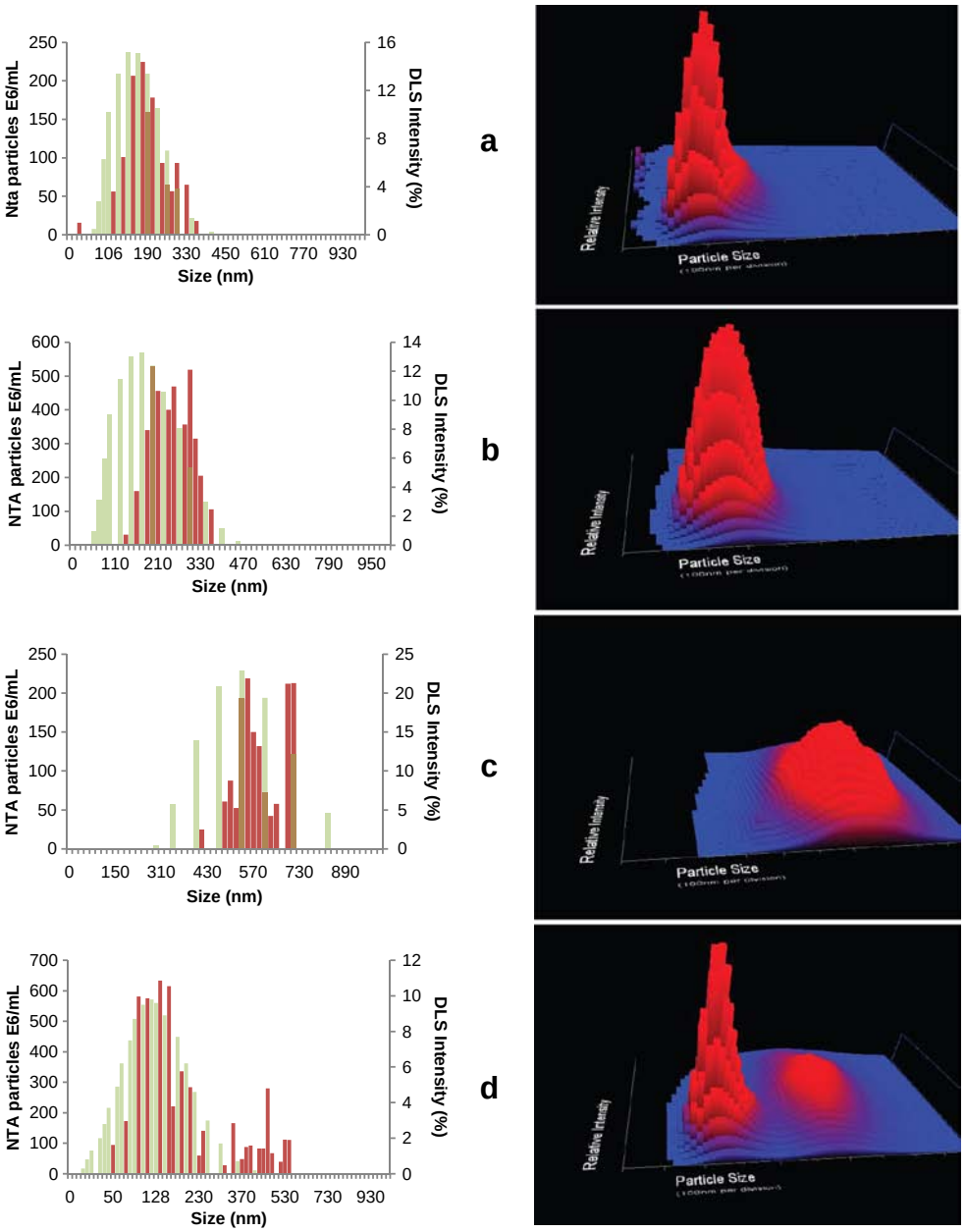

Fig. 5 Size distribution of nanoparticles obtained from NTA (*red columns*) and DLS (*green columns*) measurements with the corresponding NTA 3D graph (size *vs*. intensity *vs*. concentration). (**a**) PLGA nanocapsules (NC); (**b**) PLGA nanocapsules coated with phospholipid bilayer (NC-PC) following the lipid film hydration with the NC dispersion; (**c**) Phospholipid vesicles resulting from the lipid film hydration with water; (**d**) Mixture of PLGA nanocapsules (NC) and phospholipid vesicles (1:10 ratio v/v).

are neutral, contributing to the prompt drug release as observed.

After disruption of the bilayer, the polymer becomes available to undergo degradation and slowly release PTX, as the direct contact between water and the PLGA core increases. A sustained release of PTX is then observed. Drug release from PLGA particles depend on several factors such as the ratio between poly(lactic- acid) and poly(glycolic acid) and physical-chemical characteristics of the drug. Release mechanisms may involve transport through water-filled pores in the polymer, transport through the polymer, and dissolution of the encapsulating polymer (48). Conversely to the dynamic and faster process observed with the external envelope, drug release from polymeric nanocarriers might be explained by slowly occurring events, such as diffusion, polymer hydration, swelling and degradation, hence the prolonged release pattern for PTX from the core of NC-PCs.

This multimodal release profile represents an interesting approach for cancer treatment. Tumor growth can be effectively arrested by antiangiogenic therapy, as originally suggested by Judah Folkman (49). However, following an initial halt on vascular progression, tumors develop an adaptive response and begin re-growing, with increased invasiveness (50). Even though evasive resistance might occur, angiogenesis inhibitors are important and beneficial therapeutic options, particularly due to their reduced toxicity

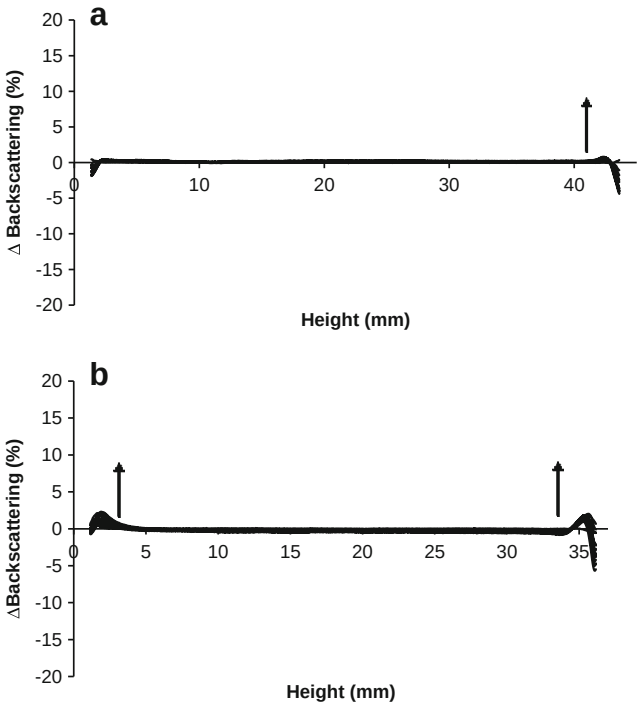

Fig. 6 Backscattering profiles of nanoparticles before (**a**) and after (**b**) coating with PC bilayer. Analysis was performed along the whole liquid column in the glass cell, at 25°C. Data was collected at 40 μm intervals and at every 20 min, during 24 h.

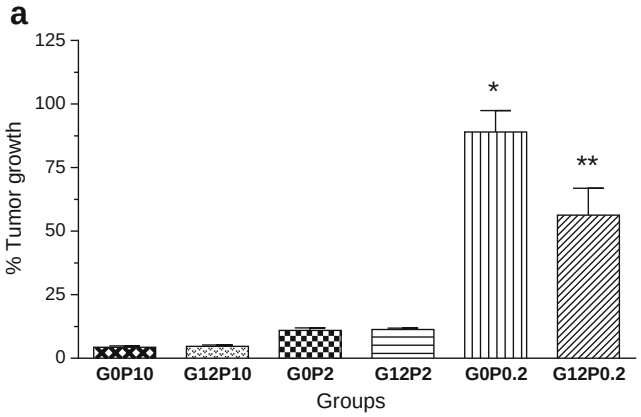

b

Group	Tumor growth inhibition (%)	Toxicity signals	
		Weight loss	Diarrhea
G0P10	96%	19.7%	+ +
G12P10	95%	22.6%	+ +
G0P2	89%	0.45%	-
G12P2	89%	1.4%	-
G0P0.2	11%	0%	-
G12P0.2	44%	1.0%	-

Fig. 8 Effect of different nanoparticle formulations of NC-PC and doses (GxPy, where x and y indicate mg/Kg/day of genistein and paclitaxel, respectively) on EAT-bearing mice. (**a**) Percentage of tumor growth, calculated in relation to the control group treated with blank nanoparticles. (**b**) Percentage of tumor inhibition and toxicity signals presented by animals from each group. Mice inoculated with EAT were treated with NC-PC for 7 days, starting 24 h after tumor inoculation (2×10^6 cells). Results are the mean ± SD for 5 mice. Statistical analysis were performed using one-way ANOVA with Tukey's multiple comparison (*$p < 0.05$).

when compared to conventional cytotoxic agents (25). The multicompartimental nanoparticles developed in this study were designed according to the current approach of combinational chemotherapy. The prompt release of the antiangiogenic drug initiates the mechanism of inhibiting neoangiogenesis while the cytotoxic drug, sustainably released from the nanoparticles in the tumoral tissue would promote its shrinkage.

Sequential antiangiogenesis and anticancer functions were also investigated by Wang and Ho (21), co-encapsulating PTX and combretastatin A4 (CA4), with promising results (11,21,51). In this work, the concept of co-encapsulation with temporal drug release was expanded to an *in vivo* experiment, with intratumoral administration of the nanomedicine,

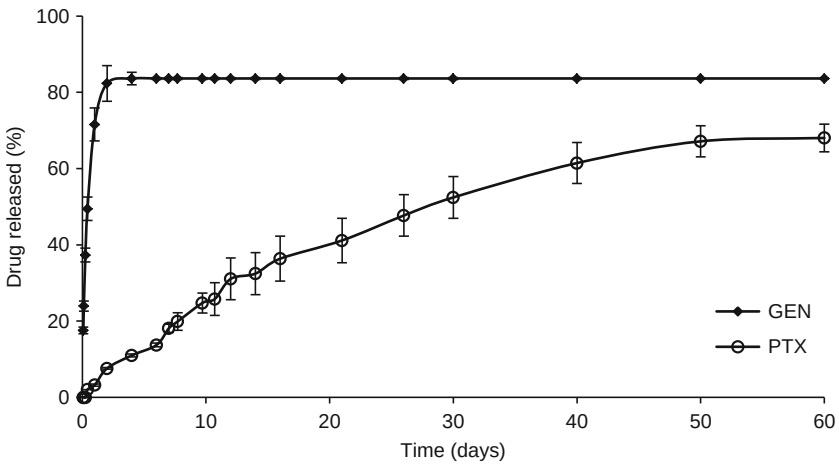

Fig. 7 *In vitro* drug release of paclitaxel (PTX) and genistein (GEN) from NC-PCs. Receptor medium was LSS 2% (w/v) separated from donor compartment by regenerated cellulose dialysis bags (MWCO 3500). Experiments were performed at 37°C during 60 days. Data represent mean ± SD ($n = 3$).

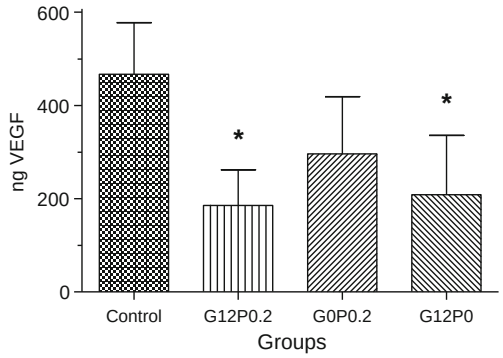

Fig. 9 Effect of treatment with nanoparticle formulations of NC-PC with 0.2 mg/Kg/day of paclitaxel (G0P0.2), or 12 mg/Kg/day genistein (G12P0), or with both drugs at the same dose (G12P0.2) on tumor levels of VEGF on day 8 post inoculation in EAT-bearing Swiss male mice. Tumor levels of VEGF were significantly ($p < 0.05$) lower than control when genistein was encapsulated in the nanoparticles. VEGF levels were measured using ELISA. Results are the mean ± SD for 5 mice. Statistical analysis were performed using one-way ANOVA with Tukey's multiple comparison (*$p < 0.05$).

demonstrating additional advantages of this nanostructured drug delivery formulation.

Ehrlich Ascites Tumor (EAT) is a mammary adenocarcinoma which following intraperitoneal transplantation readly grows in ascitic form. EAT cells are undifferentiated and exhibit a rapid growth pattern, with a very aggressive behavior (52). EAT is one of the main tumor models used to assess the activity of chemotherapeutics. One particular advantage is that tumor progression is related to the number of tumor cells transplanted. Additionally, tumor growth can be quantitatively determined by accurate cell counting systems.

When higher doses of PTX were used (10 and 2 mg/kg/day), tumor growth inhibition was 95% and 89%, respectively. At cytotoxic concentrations, PTX is able to suppress microtubule dynamics in endothelial cells, leading to cell death by apoptosis (53). As consequence of tumor shrinkage, the production of pro-angiogenic factors, such as the cytokine VEGF is markedly diminished (54). However, evident toxicity signals such as weight loss and diarrhea occurred in animals receiving 10 mg/Kg/day of PTX. Since tumor growth was strongly inhibited, the synergic effect of GEN could not be observed for groups G12P10 and G12P2. In order to verify the potential effect of this drug combination, PTX dose was reduced 10 fold, to 0.2 mg/Kg/day, allowing a certain extent of tumor progression. Since tumor growth requires angiogenesis, VEGF becomes over-expressed in a variety of neoplastic and endothelial cells (55). GEN exerts antiangiogenic activity by inhibiting

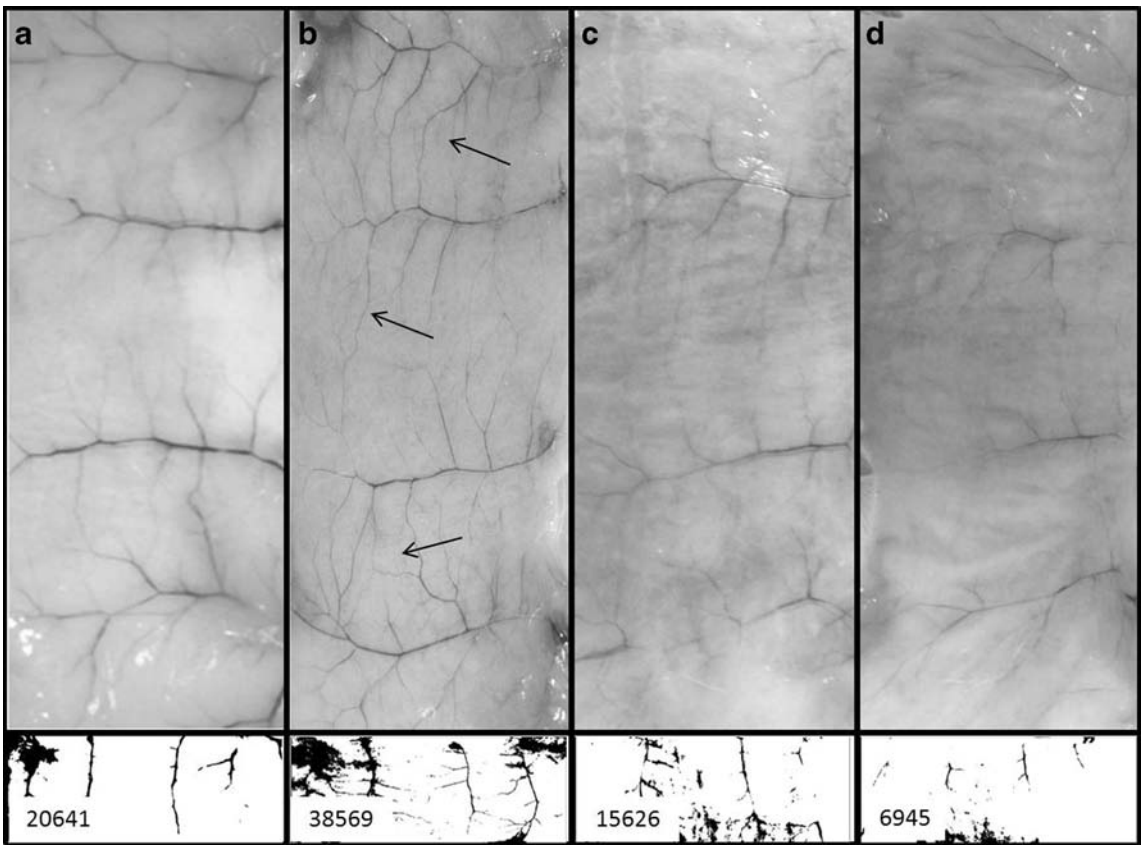

Fig. 10 Photographs of the peritoneal region of healthy (**a**) and EAT-bearing mice treated with (**b**) blank nanoparticles, (**c**) 0.2 mg/Kg/day of paclitaxel or (**d**) 0.2 mg/Kg/day of paclitaxel in association with genistein (12 mg/Kg/day) in nanoparticles. Intensity of blood vessels was obtained using Image J analysis and data are presented in each respective binary converted image. *Arrows* indicate areas of intense neovasculature.

endothelial cell activation mediated by VEGF (24). The administration of 0.2 mg/Kg/day of PTX associated with 12 mg/Kg/day of GEN inhibited tumor growth by 44%, along with a 58% decrease in VEGF levels. In contrast, nanoparticles containing only PTX, in the same dose, were able to inhibit only 11% of tumor growth. A 4-fold increase in the antitumoral activity was observed when both drugs were co-encapsulated into the multicompartimental nanoparticles, along with no evidence of toxicity.

GEN also proved its antiangiogenic effect reducing the levels of VEGF and preventing the formation of new blood vessels. GEN is a drug widely known to decrease the expression of VEGF, preventing the neoangiogenesis, which could support tumor growth (22,26,56). Although VEGF is essential for tumor growth, other angiogenic factors are produced and may compensate for the decreased levels of this cytokine (19,57), hence the need of associating GEN with cytotoxic drugs. Administration of the multicompartimental nanoparticles co-encapsulating PTX and GEN into EAT bearing mice clearly indicated an increased performance of the antitumoral activity of the nanomedicine formulation.

CONCLUSION

The development of a multicompartimental nanostructured drug delivery system consisting of a PLGA nanocapsule core and a phospholipid bilayer envelope co-encapsulating both paclitaxel and genistein was successfully achieved. Physical-chemical characteristics of these nanoparticles resulted in very high entrapment efficiency for both drugs with a sustained drug release profile in different stages. Genistein showed a potential role in tumor inhibition, preventing the formation of new blood vessels and markedly reducing VEGF levels. The antiangiogenic activity of genistein and its additional effect when associated with a low dose of paclitaxel highlight the potential of multicompartimental nanostructured drug delivery systems for the combination therapy in cancer treatment, simultaneously targeting multiple pathways towards more effective antitumoral strategies.

ACKNOWLEDGMENTS AND DISCLOSURES

This work was supported by the Brazilian research funding agencies Conselho Nacional de Desenvolvimento Científico e Tecnológico (CNPq), Financiadora de Estudos e Pesquisas (FINEP), Coordenação de Aperfeiçoamento de Pessoal de Nível Superior (CAPES), Fundação de Apoio à Pesquisa da Universidade Federal de Goiás (FUNAPE) and Fundação de Apoio à Pesquisa do Estado de Goiás (FAPEG).

REFERENCES

1. Uramoto H, Nakanishi R, Nagashima A, Uchiyama A, Inoue M, Osaki T, *et al*. A randomized phase II trial of adjuvant chemotherapy with bi-weekly carboplatin plus paclitaxel versus carboplatin plus gemcitabine in patients with completely resected non-small cell lung cancer. Anticancer Res. 2010;30(11):4695–9.
2. Pishvaian MJ, Slack R, Koh EY, Beumer JH, Hartley ML, Cotarla I, *et al*. A phase I clinical trial of the combination of imatinib and paclitaxel in patients with advanced or metastatic solid tumors refractory to standard therapy. Cancer Chemother Pharmacol. 2012;70(6):843–53.
3. Feng S-S, Zhao L, Zhang Z, Bhakta G, Yin Win K, Dong Y, *et al*. Chemotherapeutic engineering: vitamin E TPGS-emulsified nanoparticles of biodegradable polymers realized sustainable paclitaxel chemotherapy for 168 h in vivo. Chem Eng Sci. 2007;62(23):6641–8.
4. Burris 3rd HA, Dowlati A, Moss RA, Infante JR, Jones SF, Spigel DR, *et al*. Phase I study of pazopanib in combination with paclitaxel and carboplatin given every 21 days in patients with advanced solid tumors. Mol Cancer Ther. 2012;11(8):1820–8.
5. Gelderblom H, Verweij J, Nooter K, Sparreboom A. Cremophor EL: the drawbacks and advantages of vehicle selection for drug formulation. Eur J Cancer. 2001;37(13):1590–8.
6. Gradishar WJ, Tjulandin S, Davidson N, Shaw H, Desai N, Bhar P, *et al*. Phase III trial of nanoparticle albumin-bound paclitaxel compared with polyethylated castor oil-based paclitaxel in women with breast cancer. J Clin Oncol. 2005;23(31):7794–803.
7. Alberts DS, Blessing JA, Landrum LM, Warshal DP, Martin LP, Rose SL, *et al*. Phase II trial of nab-paclitaxel in the treatment of recurrent or persistent advanced cervix cancer: a gynecologic oncology group study. Gynecol Oncol. 2012;127(3):451–5.
8. Frese KK, Neesse A, Cook N, Bapiro TE, Lolkema MP, Jodrell DI, *et al*. nab-paclitaxel potentiates gemcitabine activity by reducing cytidine deaminase levels in a mouse model of pancreatic cancer. Cancer Discov. 2012;2(3):260–9.
9. Miller K, Wang M, Gralow J, Dickler M, Cobleigh M, Perez EA, *et al*. Paclitaxel plus bevacizumab versus paclitaxel alone for metastatic breast cancer. N Engl J Med. 2007;357(26):2666–76.
10. Cella D, Wang M, Wagner L, Miller K. Survival-adjusted health-related quality of life (HRQL) among patients with metastatic breast cancer receiving paclitaxel plus bevacizumab versus paclitaxel alone: results from Eastern Cooperative Oncology Group Study 2100 (E2100). Breast Cancer Res Treat. 2011;130(3):855–61.
11. Wang Z, Chui WK, Ho PC. Nanoparticulate delivery system targeted to tumor neovasculature for combined anticancer and antiangiogenesis therapy. Pharm Res. 2011;28(3):585–96.
12. Ahmed F, Pakunlu RI, Brannan A, Bates F, Minko T, Discher DE. Biodegradable polymersomes loaded with both paclitaxel and doxorubicin permeate and shrink tumors, inducing apoptosis in proportion to accumulated drug. J Control Release. 2006;116(2):150–8.
13. Guo C, Liu S, Dai Z, Jiang C, Li W. Polydiacetylene vesicles as a novel drug sustained-release system. Colloids Surf B: Biointerfaces. 2010;76(1):362–5.
14. Wang C, Wang Y, Fan M, Luo F, Qian Z. Characterization, pharmacokinetics and disposition of novel nanoscale preparations of paclitaxel. Int J Pharm. 2011;414(1–2):251–9.
15. Wu J, Lu Y, Lee A, Pan X, Yang X, Zhao X, *et al*. Reversal of multidrug resistance by transferrin-conjugated liposomes co-encapsulating doxorubicin and verapamil. J Pharm Pharm Sci. 2007;10(3):350–7.
16. Wang H, Zhao Y, Wu Y, Hu YL, Nan K, Nie G, *et al*. Enhanced anti-tumor efficacy by co-delivery of doxorubicin and paclitaxel with amphiphilic methoxy PEG-PLGA copolymer nanoparticles. Biomaterials. 2011;32(32):8281–90.

17. Cosco D, Paolino D, Maiuolo J, Russo D, Fresta M. Liposomes as multicompartmental carriers for multidrug delivery in anticancer chemotherapy. Drug Deliv Transl Res. 2011;1:66–75.
18. Bamias A, Pignata S, Pujade-Lauraine E. Angiogenesis: a promising therapeutic target for ovarian cancer. Crit Rev Oncol Hematol. 2012.
19. El-Azab M, Hishe H, Moustafa Y, el El-Awady S. Anti-angiogenic effect of resveratrol or curcumin in Ehrlich ascites carcinoma-bearing mice. Eur J Pharmacol. 2011;652(1–3):7–14.
20. Sheela ML, Ramakrishna MK, Salimath BP. Angiogenic and proliferative effects of the cytokine VEGF in Ehrlich ascites tumor cells is inhibited by Glycyrrhiza glabra. Int Immunopharmacol. 2006;6(3):494–8.
21. Wang Z, Ho PC. Self-assembled core-shell vascular-targeted nanocapsules for temporal antivasculature and anticancer activities. Small. 2010;6(22):2576–83.
22. Su SJ, Yeh TM, Chuang WJ, Ho CL, Chang KL, Cheng HL, *et al*. The novel targets for anti-angiogenesis of genistein on human cancer cells. Biochem Pharmacol. 2005;69(2):307–18.
23. Pavese JM, Farmer RL, Bergan RC. Inhibition of cancer cell invasion and metastasis by genistein. Cancer Metastasis Rev. 2010;29(3):465–82.
24. Yu X, Zhu J, Mi M, Chen W, Pan Q, Wei M. Anti-angiogenic genistein inhibits VEGF-induced endothelial cell activation by decreasing PTK activity and MAPK activation. Med Oncol. 2012;29(1):349–57.
25. Blagosklonny MV. Antiangiogenic therapy and tumor progression. Cancer Cell. 2004;5(1):13–7.
26. Hwang JT, Ha J, Park OJ. Combination of 5-fluorouracil and genistein induces apoptosis synergistically in chemo-resistant cancer cells through the modulation of AMPK and COX-2 signaling pathways. Biochem Biophys Res Commun. 2005;332(2): 433–40.
27. Li Y, Kucuk O, Hussain M, Abrams J, Cher ML, Sarkar FH. Antitumor and antimetastatic activities of docetaxel are enhanced by genistein through regulation of osteoprotegerin/receptor activator of nuclear factor-kappaB (RANK)/RANK ligand/MMP-9 signaling in prostate cancer. Cancer Res. 2006;66(9):4816–25.
28. Zhang B, Shi ZL, Liu B, Yan XB, Feng J, Tao HM. Enhanced anticancer effect of gemcitabine by genistein in osteosarcoma: the role of Akt and nuclear factor-kappaB. Anticancer Drugs. 2010;21(3): 288–96.
29. Filipe V, Hawe A, Jiskoot W. Critical evaluation of Nanoparticle Tracking Analysis (NTA) by NanoSight for the measurement of nanoparticles and protein aggregates. Pharm Res. 2010;27(5):796–810.
30. Mengual O, Meunier G, Cayre I, Puech K, Snabre P. TURBISCAN MA 2000: multiple light scattering measurement for concentrated emulsion and suspension instability analysis. Talanta. 1999;50(2): 445–56.
31. Nogueira IA, Leao AB, Vieira Mde S, Benfica PL, da Cunha LC, Valadares MC. Antitumoral and antiangiogenic activity of Synadenium umbellatum Pax. J Ethnopharmacol. 2008;120(3): 474–8.
32. Teicher BA, Sotomayor EA, Huang ZD. Antiangiogenic agents potentiate cytotoxic cancer therapies against primary and metastatic disease. Cancer Res. 1992;52(23):6702–4.
33. Folkins C, Man S, Xu P, Shaked Y, Hicklin DJ, Kerbel RS. Anticancer therapies combining antiangiogenic and tumor cell cytotoxic effects reduce the tumor stem-like cell fraction in glioma xenograft tumors. Cancer Res. 2007;67(8):3560–4.
34. Casneuf VF, Demetter P, Boterberg T, Delrue L, Peeters M, Van Damme N. Antiangiogenic versus cytotoxic therapeutic approaches in a mouse model of pancreatic cancer: an experimental study with a multitarget tyrosine kinase inhibitor (sunitinib), gemcitabine and radiotherapy. Oncol Rep. 2009;22(1):105–13.
35. Al-Ghananeem AM, Malkawi AH, Muammer YM, Balko JM, Black EP, Mourad W, *et al*. Intratumoral delivery of paclitaxel in solid tumor from biodegradable hyaluronan nanoparticle formulations. AAPS PharmSciTech. 2009;10(2):410–7.
36. Mo Y, Lim LY. Paclitaxel-loaded PLGA nanoparticles: potentiation of anticancer activity by surface conjugation with wheat germ agglutinin. J Control Release. 2005;108(2–3):244–62.
37. Vargas BA, Bidone J, Oliveira LK, Koester LS, Bassani VL, Teixeira HF. Development of topical hydrogels containing genistein-loaded nanoemulsions. J Biomed Nanotechnol. 2012;8(2):330–6.
38. Si HY, Li DP, Wang TM, Zhang HL, Ren FY, Xu ZG, *et al*. Improving the anti-tumor effect of genistein with a biocompatible superparamagnetic drug delivery system. J Nanosci Nanotechnol. 2010;10(4):2325–31.
39. Zampieri ALTC, Ferreira FS, Resende ÉC, Gaeti MPN, Diniz DGA, Taveira SF, *et al*. Biodegradable polymeric nanocapsules based on poly(DL-lactide) for genistein topical delivery: obtention, characterization and skin permeation studies. J Biomed Nanotechnol. 2013;9(8):527–34.
40. Lewis BA, Engelman DM. Lipid bilayer thickness varies linearly with acyl chain-length in fluid phosphatidylcholine vesicles. J Mol Biol. 1983;166(2):211–7.
41. Lis LJ, Mcalister M, Fuller N, Rand RP, Parsegian VA. Interactions between neutral phospholipid-bilayer membranes. Biophys J. 1982;37(3):657–65.
42. Balgavy P, Dubnickova M, Kucerka N, Kiselev MA, Yaradaikin SP, Uhrikova D. Bilayer thickness and lipid interface area in unilamellar extruded 1,2-diacylphosphatidylcholine liposomes: a small-angle neutron scattering study. BBA Biomembr. 2001;1512(1):40–52.
43. Lemarchand C, Couvreur P, Vauthier C, Costantini D, Gref R. Study of emulsion stabilization by graft copolymers using the optical analyzer Turbiscan. Int J Pharm. 2003;254(1):77–82.
44. Celia C, Trapasso E, Cosco D, Paolino D, Fresta M. Turbiscan lab expert analysis of the stability of ethosomes and ultradeformable liposomes containing a bilayer fluidizing agent. Colloids Surf B: Biointerfaces. 2009;72(1):155–60.
45. Go ML, Ngiam TL. Thermodynamics of partitioning of the antimalarial drug mefloquine in phospholipid bilayers and bulk solvents. Chem Pharm Bull. 1997;45(12):2055–60.
46. Wenk MR, Fahr A, Reszka R, Seelig J. Paclitaxel partitioning into lipid bilayers. J Pharm Sci. 1996;85(2):228–31.
47. Fahr A, van Hoogevest P, May S, Bergstrand N, Leigh MLS. Transfer of lipophilic drugs between liposomal membranes and biological interfaces: consequences for drug delivery. Eur J Pharm Sci. 2005;26(3–4):251–65.
48. Fredenberg S, Wahlgren M, Reslow M, Axelsson A. The mechanisms of drug release in poly(lactic-co-glycolic acid)-based drug delivery systems–a review. Int J Pharm. 2011;415(1–2):34–52.
49. Folkman J. Tumor angiogenesis: therapeutic implications. N Engl J Med. 1971;285(21):1182–6.
50. Paez-Ribes M, Allen E, Hudock J, Takeda T, Okuyama H, Vinals F, *et al*. Antiangiogenic therapy elicits malignant progression of tumors to increased local invasion and distant metastasis. Cancer Cell. 2009;15(3):220–31.
51. Wang Z, Ho PC. A nanocapsular combinatorial sequential drug delivery system for antiangiogenesis and anticancer activities. Biomaterials. 2010;31(27):7115–23.
52. Hartveit F, Halleraker B. Effect of subcutaneous transplants of Ehrlich carcinoma on the survival time of mice with intraperitoneal transplants of the same tumour. J Pathol. 1971;105(2):85–93.
53. Pasquier E, Honore S, Pourroy B, Jordan MA, Lehmann M, Briand C, *et al*. Antiangiogenic concentrations of paclitaxel induce an increase in microtubule dynamics in endothelial cells but not in cancer cells. Cancer Res. 2005;65(6):2433–40.
54. Shchors K, Evan G. Tumor angiogenesis: cause or consequence of cancer? Cancer Res. 2007;67(15):7059–61.

55. Roskoski Jr R. Vascular endothelial growth factor (VEGF) signaling in tumor progression. Crit Rev Oncol Hematol. 2007;62(3):179–213.
56. Banerjee S, Li Y, Wang Z, Sarkar FH. Multi-targeted therapy of cancer by genistein. Cancer Lett. 2008;269(2):226–42.
57. Yoshiji H, Harris SR, Thorgeirsson UP. Vascular endothelial growth factor is essential for initial but not continued in vivo growth of human breast carcinoma cells. Cancer Res. 1997;57(18): 3924–8.